

Original Article

Integrative analysis of lncRNA-miRNA-mRNA-associated competing endogenous RNA regulatory network involved in EV71 infection

Yanzhi Lu^{1,2}, Zhaowei Gao¹, Chong Liu¹, Min Long¹, Longfei Yang¹, Ruicheng Li¹, Ke Dong¹, Huizhong Zhang¹

¹Department of Clinical Diagnosis, Tangdu Hospital, Air Force Medical University, Xi'an, Shaanxi, China;

²Department of Microbiology and Pathogen Biology, Basic Medical School, Air Force Medical University, Xi'an, Shaanxi, China

Received March 11, 2021; Accepted May 13, 2021; Epub July 15, 2021; Published July 30, 2021

Abstract: The competing endogenous RNA (ceRNA) axis has been shown to play a critical role in the pathogenesis of various viral infections. Generally, the ceRNA network involves long non-coding RNAs (lncRNAs) that act as sponges for miRNA to regulate mRNA expression. However, no information is available regarding the involvement of ceRNA networks in Enterovirus type 71 (EV71) infections. In the present study, data obtained from Gene Expression Omnibus (GEO) database was analyzed using various bioinformatics tools. EV71 infection in rhabdomyosarcoma (RD) cells was associated with differential expression of six lncRNAs, 28 miRNAs, and 349 mRNAs. Gene function enrichment analysis suggested induction of cytoplasmic vesicle process upon EV71 infection. The ceRNA networks were constructed, in which 20 hub genes were predicted by protein-protein interaction. To confirm the MALAT1/miR-194-5p/DUSP1 ceRNA regulatory axis in EV71 infection, real-time quantitative polymerase chain reaction (qRT-PCR) and luciferase reporter assay were performed. The results of the study also revealed the involvement of the MALAT1/miR-194-5p axis in apoptosis induced by EV71 infection, while no association with autophagy was observed. Thus, the present study provided novel insights into the pathogenic mechanism of EV71 infection.

Keywords: Enterovirus type 71, competing endogenous RNA, MALAT1, miR-194-5p, apoptosis, bioinformatics

Introduction

Hand, foot and mouth disease (HFMD) is a common acute infectious disease, usually affecting infants and children under 5 years of age. It is mainly caused by Enterovirus type 71 (EV71). Since 1980s, it has been associated with periodic HFMD outbreaks in the Asia-Pacific region, Europe, and America [1]. Especially, China ranks first worldwide in the mortality and case number of HFMD [2]. Among HFMD patients, severe cases mainly caused by EV71 infection [3] suffered life-threatening complications like aseptic meningitis, encephalomyelitis, acute flaccid paralysis and even death [4]. Currently, three inactivated monovalent EV71 vaccines are approved for clinical use only in China but not in other countries or areas [5]. Other monovalent or multivalent EV71 vaccines are still under development. In addition to this, lack of complete understanding regarding the pathogenicity of this virus

makes the treatment of HFMD more challenging. Therefore, this highlights the importance of identification of key regulatory molecules involved in the pathogenicity of EV71.

In recent years, non-coding RNAs (ncRNA), including long non-coding RNA (lncRNA) and microRNAs (miRNA) have been found to be associated with pathogenic processes in several viral infections [6]. Generally, lncRNAs are ncRNAs with length >200 nucleotides that regulate several cellular processes during viral infection [7]. The miRNA molecules, about 18-25 nucleotides in length, usually regulate gene expression via binding to the 3'-untranslated region (3'-UTR) [8]. In the past few years, several studies have provided strong evidence for the role of lncRNA as sponges of miRNA. The lncRNAs bind to miRNAs and reduce the silencing effect of miRNAs on target genes, constituting a competing endogenous RNA (ceRNA) regulatory axis [6]. In viral infectious diseases,

ceRNA network in EV71 infection

Table 1. Associated data from Pubmed and Gene Expression Omnibus (GEO)

RNA	Cell line	GSE	PMID	Platform
lncRNA	RD	/	23220233	Arraystar Human lncRNA Array v2.0 slide
	RD	/	30314355	IlluminaHiSeq X Ten platform
miRNA	RD	GSE75455	26581983	Agilent-019118 Human miRNA Microarray 2.0 G4470B
mRNA	RD	GSE15323	/	Affymetrix Human Genome U133 Plus 2.0 Array
	RD	GSE103308	29696588	IlluminaHiSeq 2000

ceRNA regulatory axis usually affects virus proliferation, cellular apoptosis, and other cellular activities [6]. In a previous study by Liao et al. [9], the IRAK3-3-miR891b-GADD45 β ceRNA axis was found to have a significant effect on cellular apoptosis in EV71 infected cells. Thus, the results of this study suggested that ceRNA axes perform regulatory roles in the pathogenesis of EV71 infection.

The RNA sequencing and bioinformatics analyses are preferred methods for the prediction of the ceRNA network. In previous studies, differential expression of lncRNA [10-12] and miRNA [13] was reported in EV71 infected cells by using transcriptome sequencing. In addition to this, several lncRNA-miRNA-mRNA regulatory networks and associated biomarkers have been identified in several viral infectious diseases [14]. However, no information is available regarding the involvement of any lncRNA-miRNA-mRNA associated ceRNA network in EV71 infection.

In this study, on the basis of lncRNA sequencing results reported in previous studies [10, 11], differential expression of lncRNA was screened in EV71 infected rhabdomyosarcoma (RD) cells. RNA sequencing data of miRNA and mRNA were obtained from the Gene Expression Omnibus (GEO) database. Further, bioinformatics tools were used to screen differential expression of miRNA and mRNA in EV71 infected RD cells. Following this, the enrichment functional analyses of differentially expressed genes (DEGs) and ceRNA network construction were performed. In the end, real-time quantitative polymerase chain reaction (qRT-PCR), luciferase reporter assay, and apoptosis analysis were carried out to validate the potential ceRNA regulatory axis and its associated functions in EV71 infection. These ceRNA networks might provide better insights into the underlying pathogenic mechanism involved in EV71 infection, and thus assist in the identification of bio-

markers for diagnosis and potential drug targets for disease treatment.

Materials and methods

Data collection

The differentially expressed lncRNAs in EV71 infected RD cells were obtained from reports PMID23220233 [11] and PMID30314355 [10]. All the miRNA-seq data (GSE75455) and mRNA RNA-seq data (GSE15323 and GSE-103308) derived from EV71 infected RD cell line were downloaded from Gene Expression Omnibus (GEO) (<https://www.ncbi.nlm.nih.gov/geo/>) of National Center of Biotechnology Information (NCBI). Detailed information of platforms was listed in **Table 1**.

Identification of differentially expressed lncRNA, miRNA and mRNA

In the present study, the differentially expressed lncRNAs in previous reports [10,11] were screened. GEO2R, an interactive web tool based on limma package of R language in the GEO series, was used to screen the differential expression of miRNAs in this study. The limma package of R language was used to screen the differential expression of mRNAs. The $|\log_{2}FC| > 1$ and $P < 0.05$ were set as the cut-off criteria.

Gene function analysis

Gene Ontology (GO) is one of the bioinformatics tools used to analyze gene annotation, including biological processes (BPs), molecular functions (MFs) and cellular components (CCs) annotations. The Kyoto Encyclopedia of Genes and Genomes (KEGG) was used to determine the pathways enrichment of differentially expressed genes in cells. Gene Set Enrichment Analysis (GSEA) is an analysis method of comprehensive gene function prediction for whole

ceRNA network in EV71 infection

genome expression profile, which was used to determine the enriched signal pathways of the differentially expressed genes. The GO, KEGG and GSEA analysis were implemented through cluster Profiler package of R language.

Protein-protein interaction (PPI) network and hub genes prediction

The protein-protein interaction (PPI) network was predicted using the Search Tool for the Retrieval of Interacting Genes (STRING) online software (version: 11.0, <https://string-db.org>). The mRNA genes were put into STRING database, and gene pairs with combined scores >0.4 were selected as the candidates. Cytoscape software (version 3.7.2) was used to integrate and visualize the main part of PPI network. Next, top 20 genes of above gene pairs with the strongest correlations were analyzed by CytoHubba.

LncRNA-miRNA-mRNA interaction network

In the lncRNA-miRNA-mRNA interaction network prediction, the lncRNA-miRNA with opposite expression and miRNA-mRNA with opposite expression were used for interaction prediction. DIANA-LncBase (<https://diana.e-ce.uth.gr/lncbasev3>) and TargetScan (http://www.targetscan.org/vert_71/) were used for interaction prediction between lncRNA and miRNA or miRNA and mRNA, respectively. Finally, the lncRNA-miRNA-mRNA networks were constructed by Cytoscape software (version 3.7.2).

Cell culture and virus infection

Human rhabdomyosarcoma (RD) cell line in our laboratory was previously purchased from American Type Culture Collection (ATCC) and identified using short tandem repeats (STR) analysis by Biowing Biotechnology (Shanghai, China). The cells were cultured in Dulbecco's Modified Eagle's Medium (DMEM) supplemented with 10% heat-inactivated fetal bovine serum (FBS) at 37°C in 5% CO₂. The EV71 virus strain (strain 87-2008 Xi'an Shaanxi, GenBank Accession No. HM003207.1) obtained from the Xi'an Centre for Disease Control and Prevention, was kindly donated by Dr. Wei Ye and Dr. Min Yao. It also has been applied in several studies [15, 16]. RD cells were seeded into 24-well plates at a density of 1×10⁵ cells/well. After 24 h, cells were washed and attached with EV71 virus for 1 h at a multiple of infection (MOI) of 1 in DMEM. As a negative control,

mock treatment with EV71-free DMEM was applied to RD cells. Then, the supernatant was replaced by 2% FBS DMEM.

Cell RNA extraction and quantitative real-time PCR

At 12 h post EV71 infection, total RNAs of RD cells were extracted using Trizol reagent (Code No. 9108, Takara, Japan). Then lncRNA and mRNA were reversely transcribed using PrimeScript RT Reagent Kit (Code No. RR047A, Takara, Japan). Briefly, the gDNA Eraser was used to remove genomic DNA of 1 µg RNA. Then mRNA and lncRNA were reversely transcribed into cDNA by using PrimeScriptRT Enzyme and RT Primer Mix containing Random 6 mers and Oligo dT Primer. For miRNA, the reverse transcription was performed using Mir-X MiRNA First-Strand Synthesis Kit (Code No. RR716, Takara, Japan). In short, the miRNA was added with poly (A) tail and reversely transcribed of the first strand by using miRNA PrimeScript RT Enzyme.

Next, quantitative real-time polymerase chain reaction (qRT-PCR) was executed using Fast-Start SYBR Green Master (Roche, Switzerland) to determine the relative expression levels of lncRNA, miRNA and mRNA. The PCR reaction steps were as follows: 95°C for 2 min followed by 40 cycles of 95°C for 20 s, 60°C for 20 s and 72°C for 20 s. The following formulae were used to calculate the relative expression of genes according to Ct values: $\Delta\Delta Ct = (Ct(\text{target gene of test}) - Ct(\text{reference gene of test})) - (Ct(\text{target gene of control}) - Ct(\text{reference gene of control}))$; the relative expression level = $2^{-\Delta\Delta Ct}$. The reference genes for mRNA and miRNA were GAPDH and U6, respectively. U6 primers were provided by Mir-X miRNA First-Strand Synthesis Kit mentioned above. The primers for NEAT1, SNHG12, MALAT1, LINC02723, miR-194-5p, miR-450-5p, miR-20b-5p, DUSP1, TCF7L2 and GAPDH were listed in **Table 2** and synthesized by Sangon Biotech (Shanghai, China).

Plasmids construction and transfection

For NEAT1, SNHG12 and MALAT1 overexpression plasmids construction, lncRNA NEAT1, SNHG12 and MALAT1 fragments were amplified from cDNA of RD cells and then cloned into plasmid pcDNA3.1 by using molecular cloning technique.

ceRNA network in EV71 infection

Table 2. Primers used for qRT-PCR

Gene		Sequence (5' to 3')
NEAT1	Forward	GACCTCTCACCTACCCACCT
	Reverse	TCCCAGCGTTTAGCACAACA
SNHG12	Forward	GAAAAAGCACACCAGCTATTGG
	Reverse	CGGGATCTCTGTAGACTAAGTCAGT
MALAT1	Forward	CTAAGGTCAAGAGAAGTGTCAG
	Reverse	AAGACCTCGACACCATCGTTAC
miR-194-5p	Forward	TGTAACAGCAACTCCATGTGGA
miR-450-5p	Forward	TTTTGCAATATGTTCTGAATA
miR-20b-5p	Forward	CAAAGTGCTCATAGTGCAGG
DUSP1	Forward	TCCCCTGAGTACTAGCGTCC
	Reverse	TGGGACAATTGGCTGAGACG
TCF7L2	Forward	GGCAAGATGGAGGGCTCTTT
	Reverse	CGCAGAGTAATGTGTGCTGC
GAPDH	Forward	GGAGCGAGATCCCTCCAAAAT
	Reverse	GGCTGTTGTCATACTTCTCATGG

RD cells were seeded in 24-well plates as described above. When cells reached 50% confluency, the transfections of plasmids and miRNA mimics were performed by using Lipofectamine 2000 reagent (Cat No. 11668-027, Invitrogen, CA) according to the manufacturer's protocol. At 48 h after transfection, the total RNAs of cells were extracted. The miR-194-5p and DUSP1 relative expression levels were measured using qRT-PCR as described above. At 36 h after transfection, the cells were collected for apoptosis detection.

Luciferase reporter assay

The luciferase reporter plasmids for wild-type MALAT1 (pGL3-MALAT1), mutant MALAT1 (pGL3-MALAT1mut), wild-type DUSP1 3'-UTR (pGL3-DUSP1) and mutant DUSP1 3'-UTR (pGL3-DUSP1mut), as well as miR-194-5p mimics, were synthesized by Sangon Biotech (Shanghai, China). For luciferase reporter assay, HEK293 cells were seeded into 24-well and transiently cotransfected with pGL3 plasmids, pRL-TK-Renilla, miR-194-5p mimics and miR mimics NC. After 48 h, the luciferase activities in cells were detected by using Dual luciferase reporter assay kit (Cat No. E1910, Promega, USA).

Cell apoptosis assay

RD cells in 24-well plates were treated with EV71 infection, overexpression plasmids trans-

fection or miR-194-5p mimics transfection, respectively. At 12 h post EV71 infection, 36 h post plasmids transfection or miRNA mimics transfection, cells were collected for apoptosis detection using an apoptosis detection kit (Cat No. KGA108, Keygen, China). Briefly, cells were digested with trypsin followed by PBS washing. Then, cells were resuspended in binding buffer and added with Annexin and PI. The apoptosis detection was performed on a FACSCalibur™ system (BD Biosciences, San Jose, CA, USA).

Western blot

The RD cells were treated with EV71 infection for 12 h, pcDNA-MALAT1 transfection for 36 h or miR-194-5p mimics transfection for 36 h. Then, the proteins were collected for Western blot analysis. Briefly, 10 µg proteins were uploaded onto sodium dodecyl sulfate polyacrylamide gel electrophoresis (SDS-PAGE) and then transferred to polyvinylidene fluoride (PVDF) membrane. After blocked by 5% milk in TBST, membranes were incubated with specific primary antibodies, such as rabbit polyclonal antibody against LC3B (~18 kDa for LC3-I and ~16 for LC3-II, Cat No. NB100-2220, Novus, USA), rabbit polyclonal antibody against p62 (~62 kDa, Cat No. NBP1-48320, Novus, USA) and mouse monoclonal antibody against β-actin (~42 kDa, Cat No. ab6276, Abcam, UK). The goat anti-mouse or goat anti-rabbit antibodies conjugated with horseradish peroxidase (Cat No. ZB-2305 and ZB-2301, Zhongshanjinqiao, China) were used as secondary antibodies. The blots were detected with chemiluminescent substrates (ECL, Millipore, USA) and quantified using ImageJ software (version 1.52a).

Statistical analysis

The significant difference analysis of lncRNA, miRNA, mRNA expression, apoptosis alteration, and Western blot quantification were performed using GraphPad Prism 7.0. The Student's t-test was used for comparison between two groups, and the analysis of variance (ANOVA) was used for comparison among multiple groups. A $P < 0.05$ was regarded as significant difference. The asterisk (*) indicates significant difference between two groups (* $P < 0.05$, ** $P < 0.01$, *** $P < 0.001$).

ceRNA network in EV71 infection

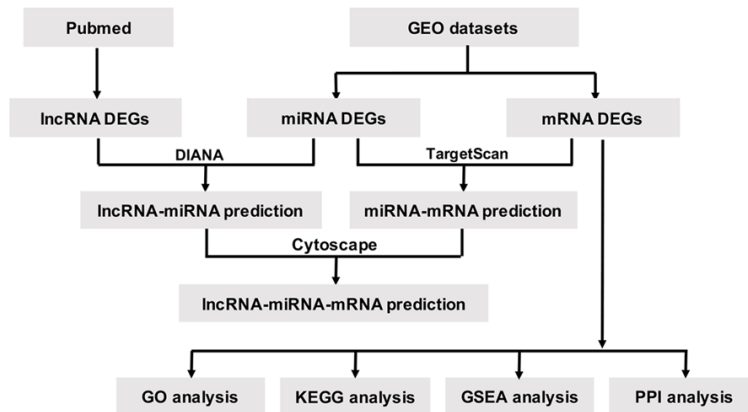


Figure 1. Flowchart for construction of ceRNA network and analysis of gene functions in EV71 infected RD cells.

Results

Identification of differentially expressed lncRNA, miRNA and mRNA in EV71 infected RD cells

The present study screened the differential expression of lncRNA, miRNA, and mRNA in RD cells infected with EV71, with the aim to identify the ceRNA regulatory axis involved in EV71 infection. The steps followed in the analysis are summarized as a flowchart in **Figure 1**. Initially, the lncRNA, miRNA, and mRNA expression profiles for RD cells infected with EV71 were obtained from PubMed (PMID23220233 and PMID30314355 for lncRNA) and GEO datasets (GSE75455 for miRNA and GSE15323/GSE103308 for mRNA). The detailed information was shown in **Table 1**. As shown in **Figure 2A** and **Table 3**, five lncRNAs were found to be upregulated, while one lncRNA was downregulated in the dataset obtained from PubMed. For GSE datasets, the GEO2R tool and limma package of R language were used for the screening. In the case of miRNAs, 10 and 18 miRNAs were found to be upregulated and downregulated, respectively (**Figure 2B**; **Table 4**). Further analysis revealed 46 upregulated mRNAs and 303 downregulated mRNAs (**Figure 2C**; **Table 5**). Heatmaps representing these differentially expressed miRNA and mRNA are shown in **Figure 2D, 2E**. Thus, the information obtained regarding the differentially expressed lncRNA, miRNA, and mRNA might provide potential leads for unraveling the pathogenic mechanism involved in EV71 infection.

Gene function analysis of DEGs

In order to analyze the possible biological functions for the differentially expressed mRNAs and their associated pathways, Gene ontology (GO) and KEGG analyses were performed using clusterProfiler package. GO analysis showed enrichment of DEGs into three main domains, namely biological processes (BPs), cellular components (CCs), and molecular functions (MFs). Among the BPs, the most significant

enrichment was reported for blood circulation and circulatory system (**Figure 3A**). In the case of CCs, the most significant enrichment was obtained for cytoplasmic vesicle lumen (**Figure 3B**). For MFs, ATPase activity coupled to transmembrane movement of substance was found to be most significantly enriched (**Figure 3C**). Further, KEGG pathway analysis for EV71 infected RD cells showed enrichment of DEGs in the cGMP-PKG signaling pathway (**Figure 3D**). All these results suggested that EV71 infection was accompanied by certain transmembrane movements in the vesicle lumen, like apoptosis and autophagy.

Gene set enrichment analysis (GSEA) for DEGs associated with EV71 infection

In order to explore the biological functions of the DEGs associated with EV71 infection in RD cells, GSEA was performed using clusterProfiler. As shown in **Figure 4A, 4B**, most of the upregulated genes were found to be associated with hypoxia and TNF- α signaling pathway via NF- κ B. All these results indicated that activation of these pathways posts EV71 infection in RD cells.

PPI network analysis of DEGs in ceRNA networks

STRING software was used to predict the protein-protein interaction (PPI) among mRNA molecules in the ceRNA network. The results for PPI network analysis are shown in **Figure 5A**. Following this, the top 20 hub genes related to EV71 infection, namely STAT3, FOS, JUN, EGR1,

ceRNA network in EV71 infection

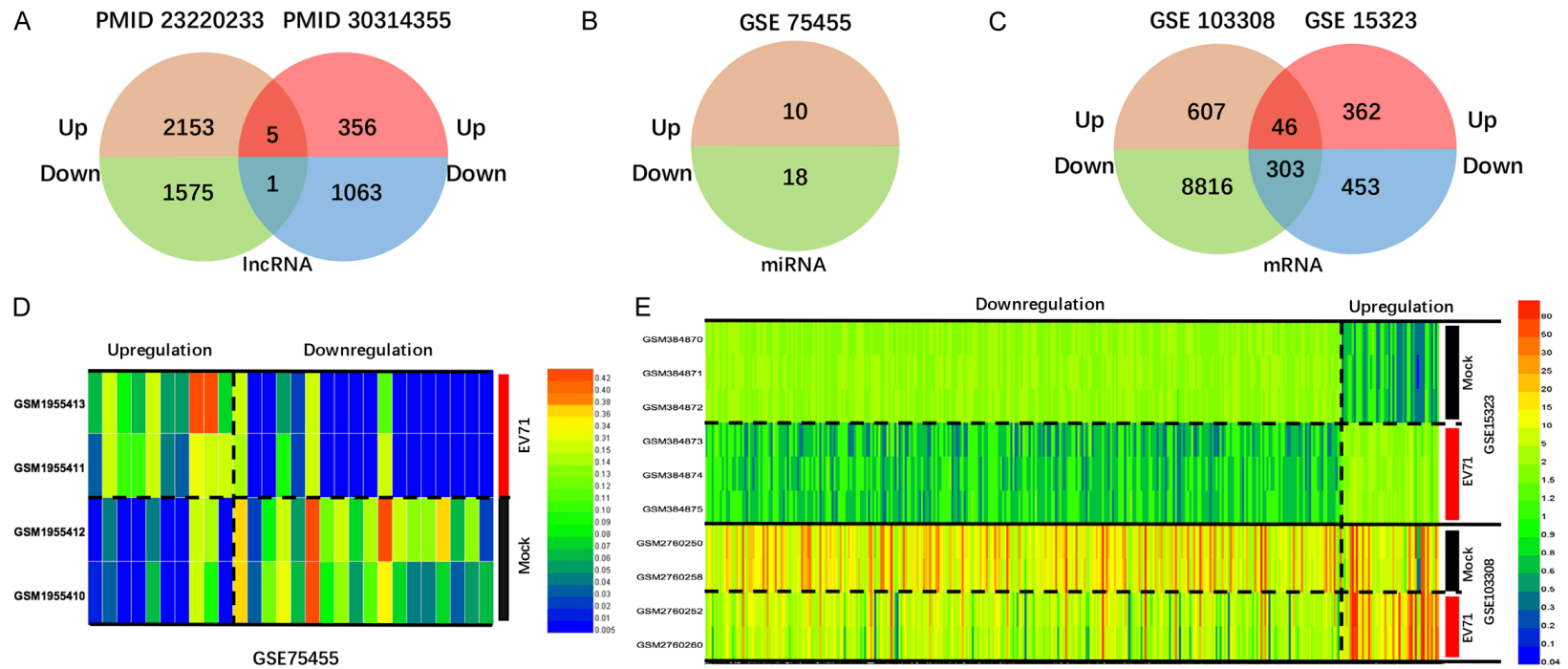


Figure 2. Venn diagrams and heat maps of differentially expressed lncRNA, miRNA and mRNA in data obtained from NCBI. A. Venn diagram presenting differentially expressed lncRNA from literature PMID23220233 and PMID30314355. B. Venn diagram presenting differentially expressed miRNA from GSE75455. C. Venn diagram presenting differentially expressed mRNA from GSE15323 and GSE103308. D. Heatmap plot presenting differentially expressed miRNA from GSE75455. E. Heatmap plot presenting differentially expressed mRNA from GSE15323 and GSE103308.

ceRNA network in EV71 infection

Table 3. Differentially expressed lncRNAs in PMID23220233 and PMID30314355

Upregulation	Downregulation
NEAT1, SNHG12, MALAT1, AC008443.5, AC003092.1	LINC02723

CYR61, DUSP1, CTGF, CDC42, PTPN11, GSK3B, NFKBIZ, REL, AKT3, MAFF, GNAQ, AKAP13, ACTR2, ARHGAP35, ADAM10, and TCF7L2, were analyzed using CytoHubba plugin of Cytoscape (**Figure 5B**). These genes might play a pivotal role in the pathogenesis of EV71 infection.

Prediction of lncRNA-miRNA-mRNA network

A competing endogenous RNA (ceRNA) network was constructed to gain detailed insights into the key regulatory functions of these RNAs. DIANA software was used to predict interactions between lncRNA and miRNA. Further, the interaction between miRNA and target mRNA was predicted using TargetScan. As shown in **Figure 6A**, the upregulated lncRNA, downregulated miRNA, and upregulated mRNA constituted an upregulated ceRNA network. In addition to this, a downregulated ceRNA network was also observed, comprising downregulated lncRNA, upregulated miRNA and downregulated mRNA (**Figure 6B**).

Verification of lncRNA, miRNA and mRNA expression

The expressions of predicted lncRNA, miRNA, and mRNA in EV71 infected RD cells were confirmed using qRT-PCR. In EV71 infected RD cells, the relative expressions of lncRNA nuclear-enriched abundant transcript 1 (NEAT1), small nucleolar RNA host gene 12 (SNHG12), and metastasis-associated lung adenocarcinoma transcript 1 (MALAT1) were found to be significantly higher as compared to those in the control cells. In comparison to these, no significant changes were observed in the expression of LINC02723 (**Figure 7A**). For miRNA expression, miR-194-5p, miR-450b-5p, and miR-129-5p were found to be significantly downregulated, while the expression of miR-20b-5p, miR-28-3p, and miR-363-3p remained unaltered (**Figure 7B**). Since the expression level of miR-194-5p reduced by nearly ten folds during EV71 infection, it was interesting for us to determine the expression of its potential target

genes, dual specificity protein phosphatase 1 (DUSP1) and transcription factor 7-like 2 (TCF7L2). As shown in **Figure 7C**, the expression of DUSP1, one of 20 hub genes, was significantly

upregulated after EV71 infection (**Figure 7C**). All these results indicated possible activation of an lncRNA/miR-194-5p/DUSP1 regulatory pathway in EV71 infection.

Validation of lncRNA/miR-194-5p/DUSP1 ceRNA axis

The potential activation of lncRNA/miR-194-5p/DUSP1 ceRNA axis was verified by overexpression of lncRNA NEAT1, SNHG12, and MALAT1 in RD cells. The overexpression of MALAT1 was accompanied by an increased expression of DUSP1 (**Figure 8A**); however, both NEAT1 and SNHG12 did not show any effect on DUSP1 expression (**Figure 8B**). Besides this, the overexpression of miR-194-5p resulted in a reduction in DUSP1 expression, indicating that DUSP1 might be one of the targets of miR-194-5p (**Figure 8C**). Further, the RNA interaction in MALAT1/miR-194-5p/DUSP1 axis was validated using luciferase reporter assay, based on the binding sites (**Figure 8D**). As shown in **Figure 8E**, miR-194-5p mimics significantly reduced the luciferase activity of wild-type MALAT1; however, no effect was observed in the case of mutant MALAT1. In addition to this, miR-194-5p mimics significantly reduced the luciferase activity of DUSP1 having wild-type 3'-UTR, but no effects were reported for DUSP1 with mutant 3'-UTR (**Figure 8E**). Thus, all these results suggested the existence of a MALAT1/miR-194-5p/DUSP1 regulatory axis for EV71 infection in RD cells.

MALAT1/miR-194-5p mediated apoptosis, but not autophagy, in EV71 infected RD cells

The results for GO analysis showed enrichment of DEGs in cytoplasmic vesicle lumen component and transmembrane movement function (**Figure 3B, 3C**), suggesting that EV71 infection might be associated with cellular apoptosis and autophagy. As shown in **Figure 9A**, EV71 infection was associated with a higher number of apoptotic RD cells, especially in early apoptosis, as compared to the control cells without any infection. Since EV71 infection resulted in

ceRNA network in EV71 infection

Table 4. Differentially expressed miRNAs in GSE75455

Upregulation	Downregulation
miR-624, miR-20b-5p, miR-191, miR-452, miR-513b, miR-195, let-7g, miR-493, miR-369-3p, miR-637	miR-28-3p, miR-363-3p, miR-632, miR-194-5p, miR-571, miR-520f, miR-129, miR-550, miR-650, miR-30c, miR-639, miR-223, miR-616-5p, miR-302b, miR-450b-5p, miR-873, miR-563, miR-199b-5p

Table 5. Differentially expressed mRNAs in GSE103308 and GSE15323

Upregulation	Downregulation
ADAMTS1, ADM, AKAP13, ARRDC3, BRF2, CDC42, CHD2, CITED2, CTGF, CXCL2, CXCL3, CYR61, DUSP1, EGR1, EIF4B, FAF2, FOS, GMEB1, HES1, JUN, MAFF, MDM4, MGEA5, MTPAP, MYLIP, NFKB2, NFKBIZ, NIPBL, NSF, PAPOLG, PIM1, QTRTD1, REL, RIT1, SARS, SGPL1, SLC2A3, SLC44A2, STAT3, TCF7L2, TOP1, TXNIP, UGCG, XBP1, ZNF350, ZNF367, ZNF441, ZNF844	ABI2, ACADSB, ACTR2, ADAM10, ADAM12, ADRBK2, AGPAT5, AGPS, AKT3, ANKFY1, ANKRD50, APPBP2, APPL1, ARFGEF1, ARHGAP35, ARHGAP5, ATAD2B, ATL3, ATP2B1, ATP6V1C1, ATR, AVL9, BAG2, BBX, BCL2, BCL2L11, BIRC6, BLOC1S6, BMPR2, BNIP2, BRCA2, BRCC3, CALD1, CASK, CBX3, CCDC6, CDC14B, CDK1, CDK19, CEP68, CEPT1, CERS6, CHML, CHRM3, CLCN5, CLOCK, CNOT6, COL11A1, COL12A1, CRK, DBT, DCAF10, DCTN5, DENND5B, DICER1, DMXL1, DNAJC10, DNAJC13, DNM3OS, DOCK1, DOCK9, DPP8, DYNC1LI2, DYNLL2, DZIP3, EIF3F, EIF3M, ELK4, EML1, EML4, EPHA7, ERCC6L2, ESYT2, FAM102B, FAM161A, FAM178A, FAM208A, FAM20B, FAM63B, FAR1, FAT3, FBXO34, FBXO5, FBXW2, FGD4, FKBP14, FKBP7, FOXN3, GALNT7, GAS1, GJC1, GLCE, GLS, GNAQ, GNB4, GPAM, GPATCH2L, GPR155, GSK3B, GSPT1, GTF3C4, GUCY1A2, GXYLT1, H2AFY, HDGFRP3, HEXIM1, HOOK3, HS2ST1, HS6ST2, HSDL1, HSP90B1, IFRD1, IL17RD, IMPAD1, IREB2, IVNS1ABP, JPX, KANSL1L, KCNJ6, KCTD12, KCTD3, KDM1B, KDSR, KIAA0368, KIAA1244, KIAA1715, KIDINS220, KRCC1, LAMB1, LAMP2, LARP4, LEPROT, LIFR, LMAN1, LMBR1, LMO4, LRIG2, LRP8, LRRC58, MAML2, MAN1A2, MAPK9, MARS2, MED13, METTL15, MFSD8, MIB1, MKLN1, MMP16, MOB1B, MPHOSPH9, MRPL42, MSRB3, MTX3, MYO5A, MYO5B, MYOF, NAA50, NEDD1, NLN, NT5DC1, NUDT4, NUFIP2, NUS1, NXPE3, ONECUT2, PAFAH1B1, PALLD, PANK3, PAPOLA, PARP14, PARVA, PBRM1, PCDH9, PCNX, PDZD8, PGRMC2, PHF20L1, PHLDA1, PHLDB2, PIGW, PIK3C2A, PLA2G12A, PMS1, POLR1B, PPARGC1B, PPFIA1, PPP1R3D, PPP6R3, PRKAA1, PRKDC, PRKRA, PRPF4B, PSEN1, PSMA5, PSME4, PTP4A1, PTPN11, PTPRD, QKI, QSER1, RAB22A, RANBP2, RASA1, RBFOX1, RBL1, REEP5, RGM B, RNF217, ROCK2, RPRD1A, RPS24, RPS6KA3, RRP15, SACS, SCARB2, SCN9A, SEMA6A, SENP6, SESN3, SFXN1, SH3GLB1, SIKE1, SLC30A7, SLC44A1, SLC4A7, SLC5A3, SLC7A2, SLITRK5, SMAD5, SMC6, SMCHD1, SMEK2, SMURF2, SNTB2, SNX1, SNX5, SOCS6, SOGA1, SOX11, SPATA6, SPTSSA, SSR1, ST8SIA4, STRBP, STRN, SUPT16H, SUV420H1, SVIL, SYNPO2, THNSL1, TM9SF3, TMED5, TMEM181, TMEM245, TMEM30A, TMEM5, TMTC1, TOR1AIP2, TPD52, TRERF1, TRIM13, TRIP11, TTC37, TTL7, TUG1, TULP4, TXLNG, UBE2K, UBE2V2, UBE4B, UBR3, UBXN4, USP13, USP14, USP24, USP34, USP46, USP9X, UTP23, VCAN, VKORC1L1, VPS13B, WDFY2, WDR3, WDR89, WHSC1L1, YES1, ZBTB37, ZBTB44, ZKSCAN1, ZMYM4, ZNF22, ZNF260, ZNF431, ZNF518B, ZNF566, ZNF594, ZNF623, ZNF704, ZNF770, ZNF830, ZXDC

increased expression of MALAT1, the study also examined effect of MALAT1 and miR-194-5p on cellular apoptosis. The overexpression of MALAT1 promoted both early and late apoptosis (**Figure 9B**). In comparison to this, the accumulation of miR-194-5p inhibited both of early and late apoptosis (**Figure 9C**). Thus, it can be concluded that EV71 infection promoted cell apoptosis probably via MALAT1/miR-194-5p axis.

In order to explore whether MALAT1/miR-194-5p mediates EV71-induced autophagy, we used Western blot to detect the key marker proteins of autophagy, such as LC3 and p62. The results showed that EV71 infection induced the accumulation of LC3-II protein and reduction of p62 protein (**Figure 9D**), indicating that autophagy was activated. However, the overexpression of MALAT1 and miR-194-5p did not alter the protein levels of LC3-II and p62 (**Figure 9E**,

ceRNA network in EV71 infection

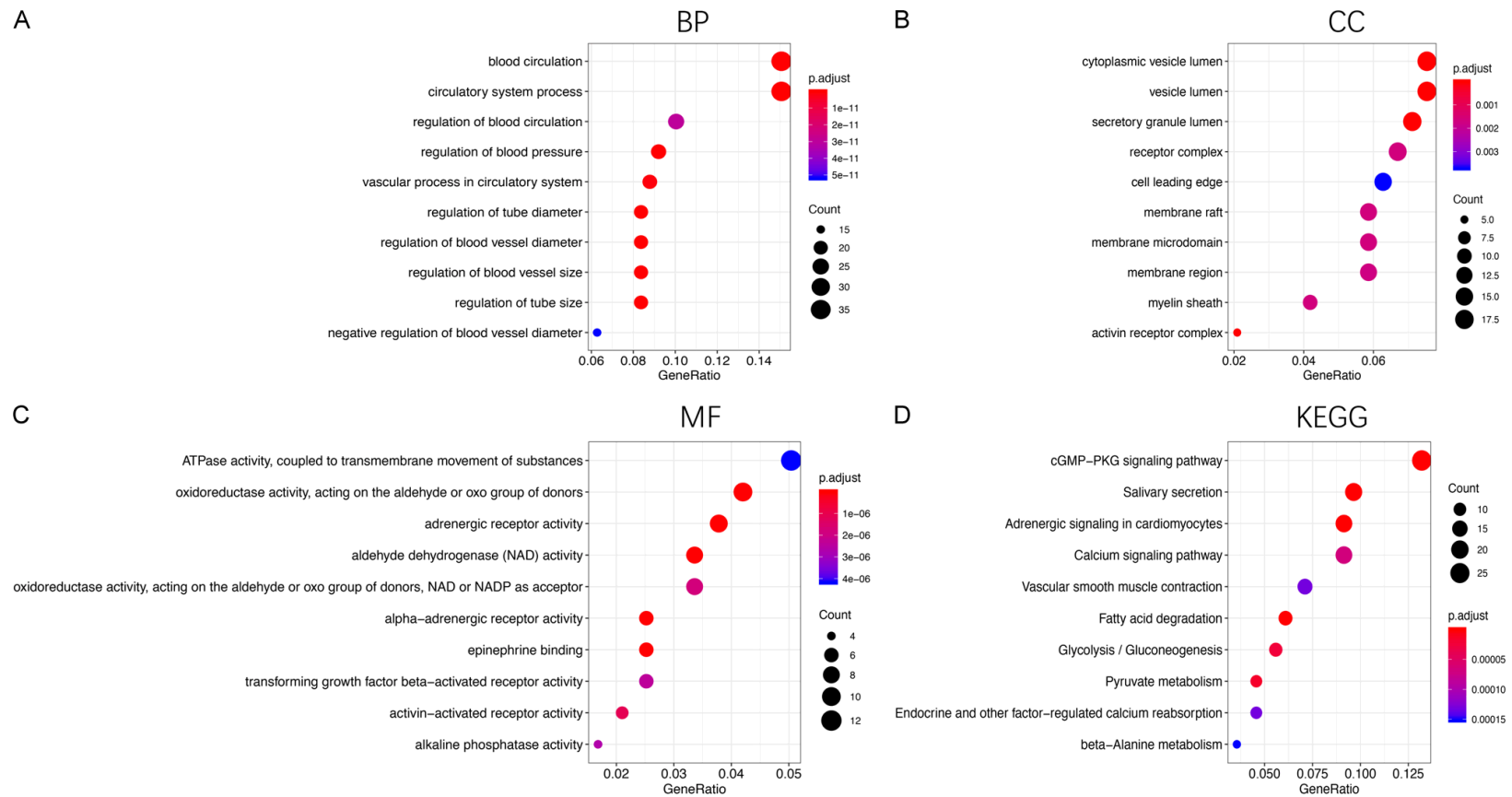


Figure 3. Gene ontology (GO) and pathway enrichment analyses for differentially expressed genes (DEGs) in EV71 infected RD cells. (A) Biological processes (BPs), (B) cellular components (CCs), and (C) molecular functions (MFs) analyses for DEGs. (D) Kyoto Encyclopedia of Genes and Genomes (KEGG) analyses for DEGs.

ceRNA network in EV71 infection

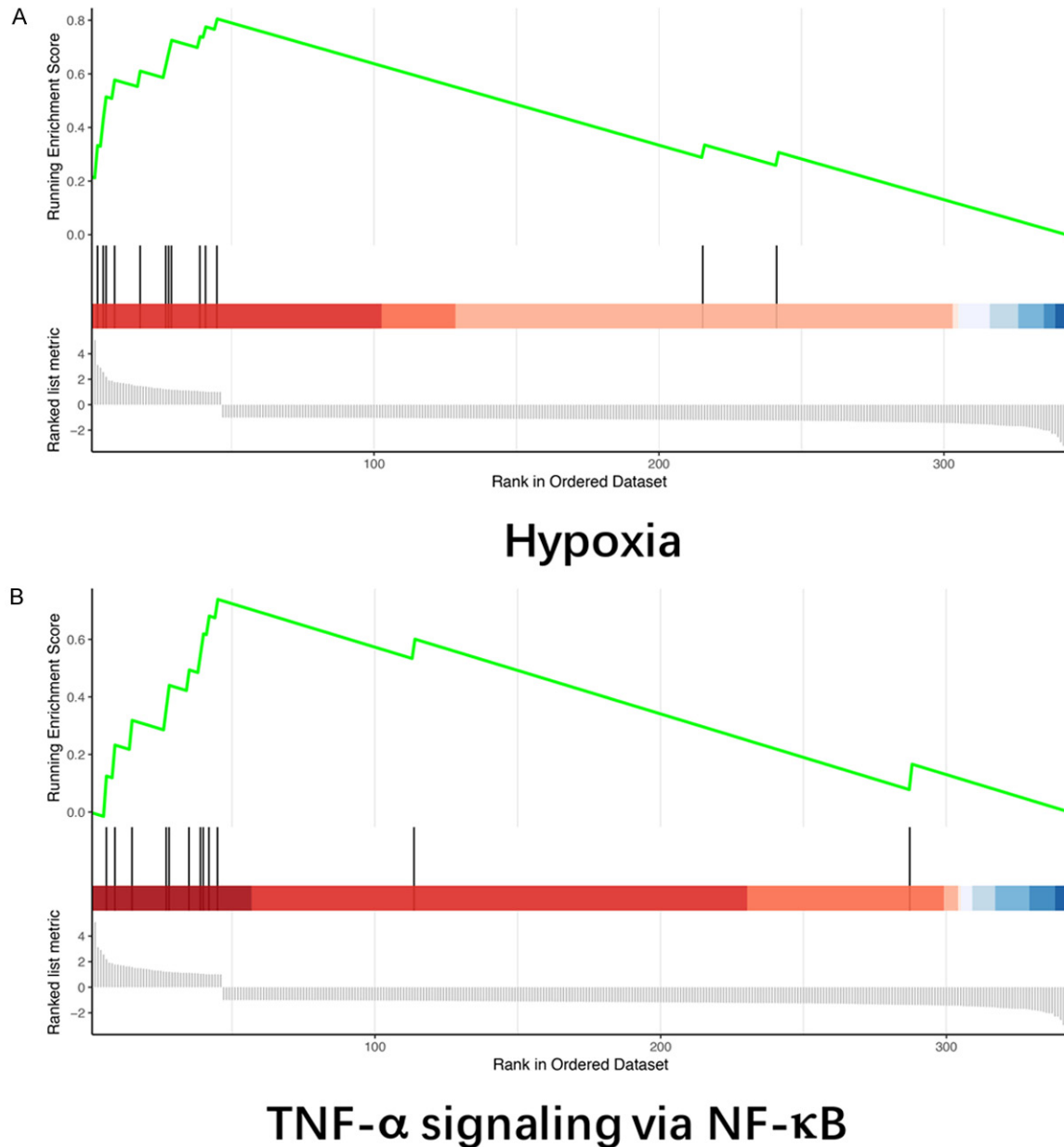


Figure 4. GSEA showed enrichment of upregulated genes in hypoxia signaling pathways (A) and TNF- α signaling pathway (B) via NF- κ B.

9F). Therefore, we conclude that the MALAT1/miR-194-5p axis did not mediate autophagy induced by EV71 infection.

Discussion

The present study explored the differential expression of genes in RD cells infected with EV71, the main causative agent of HFMD. GO, KEGG, and GSEA analyses revealed enrichment of the DEGs in cytoplasmic vesicle lumen, ATPase activity coupled to transmembrane

movement of material, and TNF- α signaling pathway. Among 20 hub genes identified using PPI network analysis, DUSP1, STAT3, FOS, and EGR1 were the main transcription factors involved in gene regulation, apoptosis, autophagy, and immune response induced by EV71 infection [17-19]. Therefore, all these observations indicated activation of antiviral activities and vesicle-related biological activities such as apoptosis and autophagy upon EV71 infection, which might further play an important role in the occurrence and pathogenesis of HFMD.

ceRNA network in EV71 infection

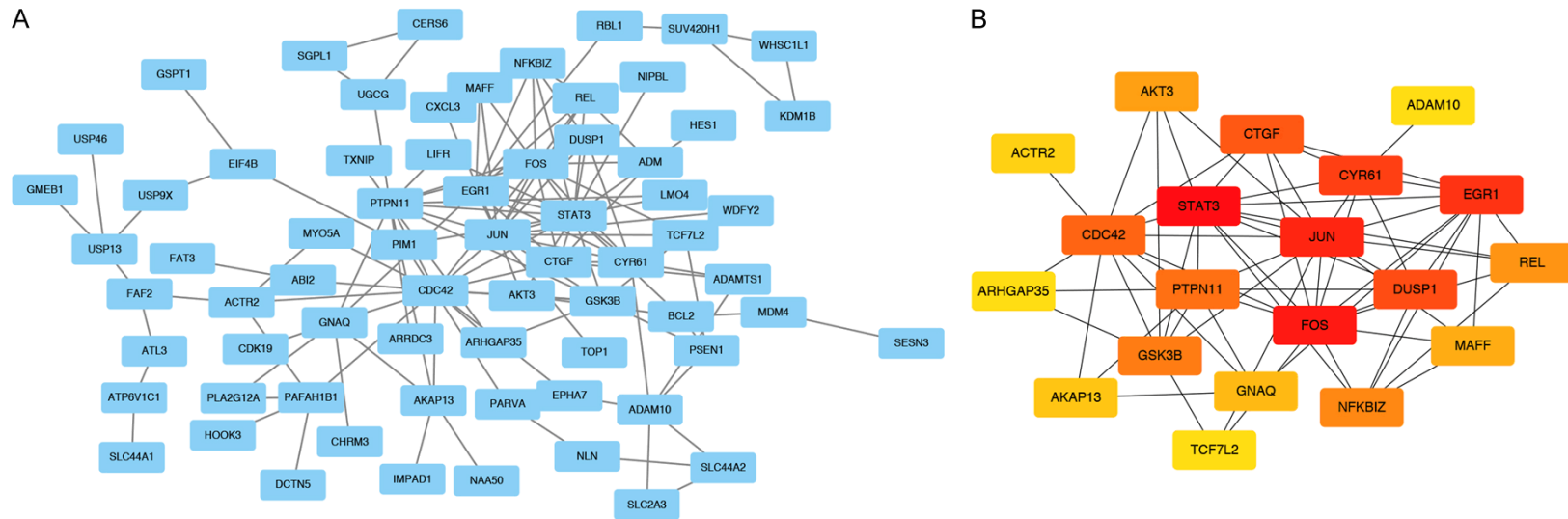
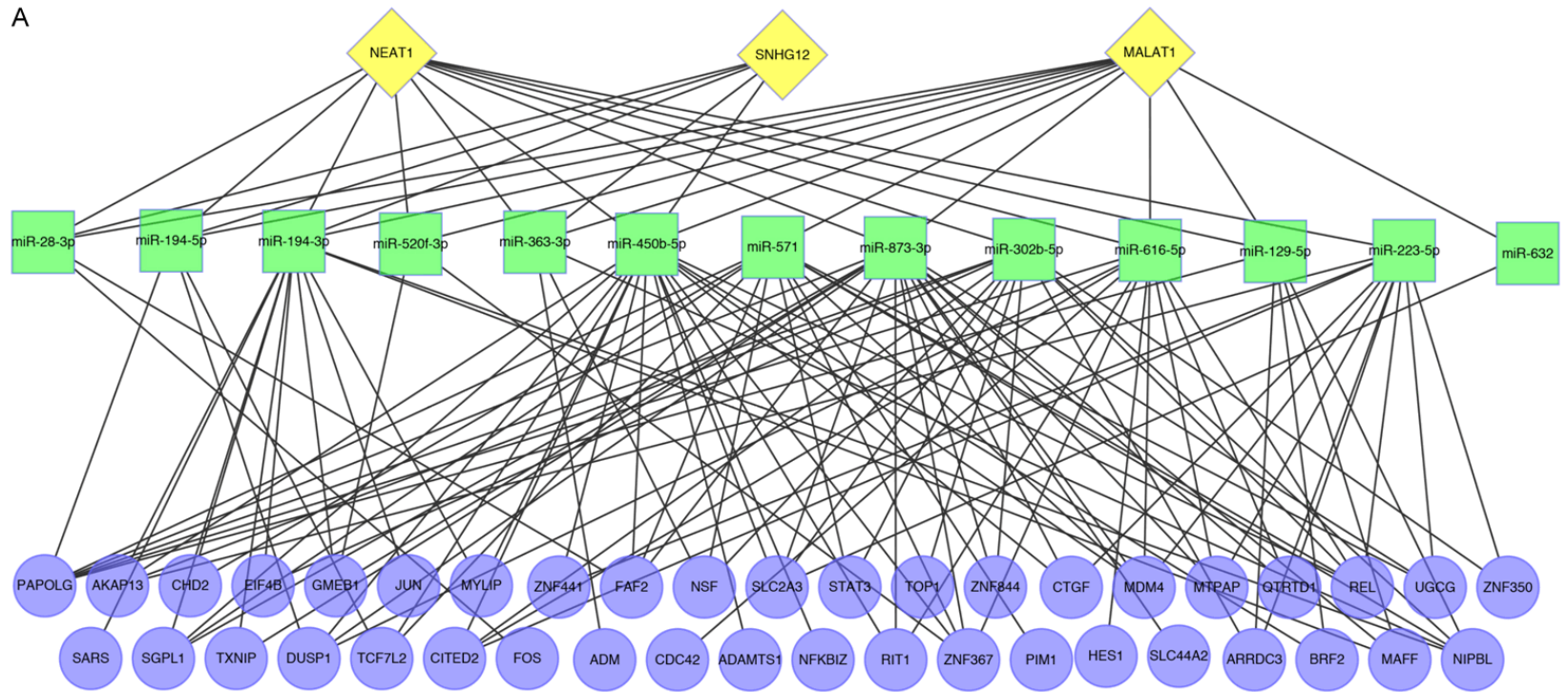


Figure 5. PPI networks construction. A. PPI network of mRNAs built by STRING software. B. Top 20 genes of above genes with the strongest correlations analyzed by CytoHubba.

ceRNA network in EV71 infection

A



ceRNA network in EV71 infection

B

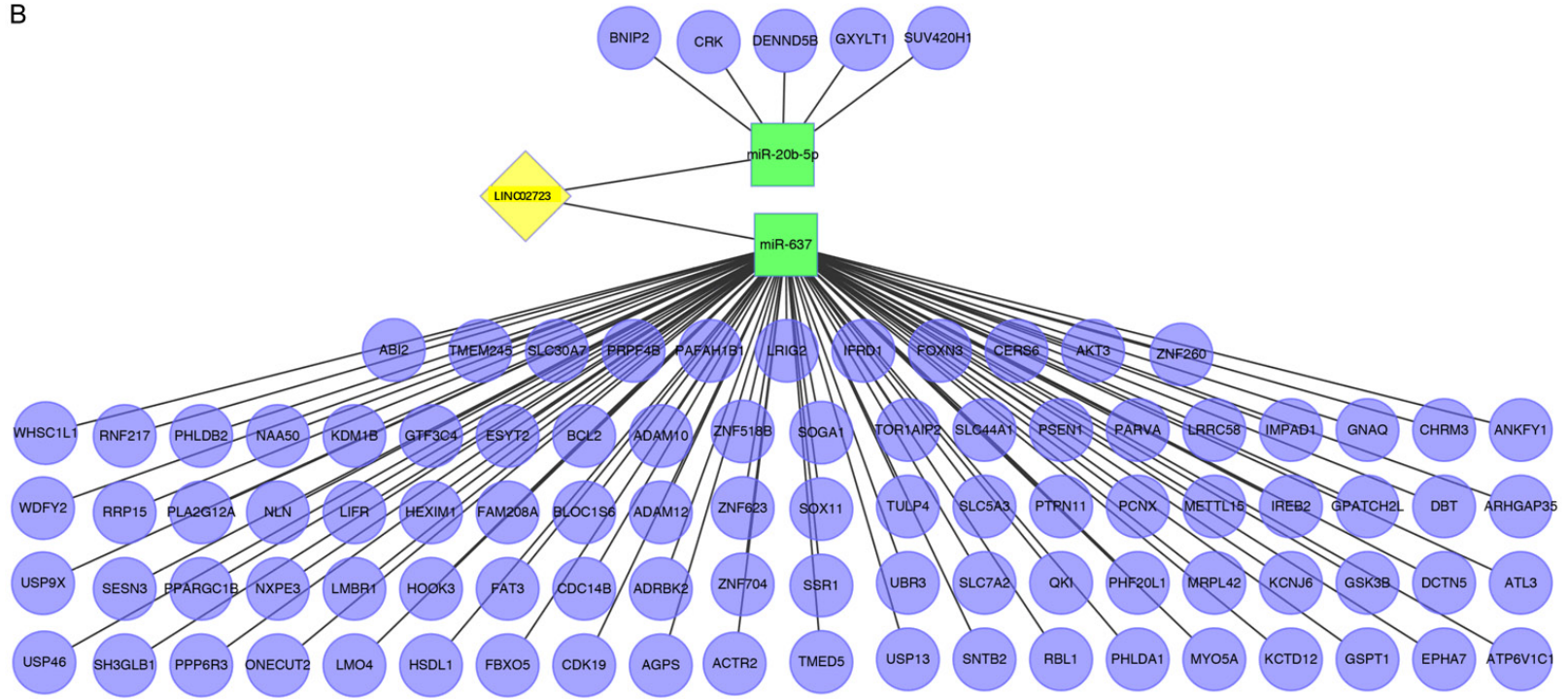
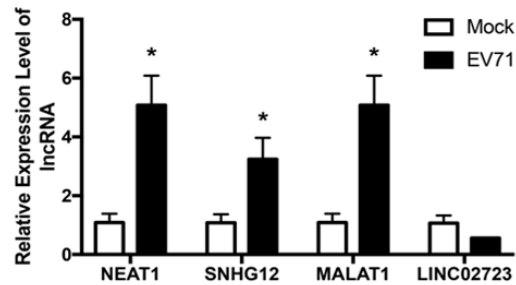
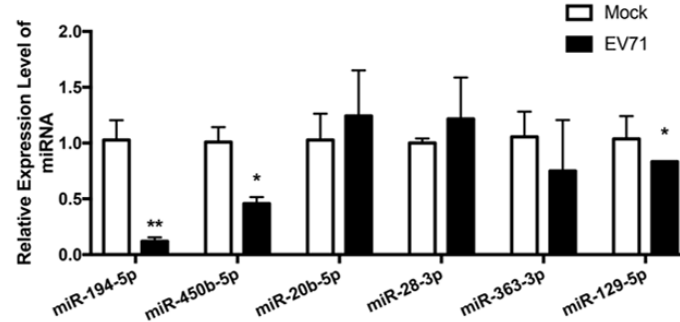


Figure 6. Prediction of lncRNA-miRNA-mRNA network of EV71 infection in RD cells. A. The ceRNA network of upregulated lncRNA. B. The ceRNA network of down-regulated lncRNA. The yellow, green and purple nodes represented lncRNA, miRNA, and mRNA, respectively.

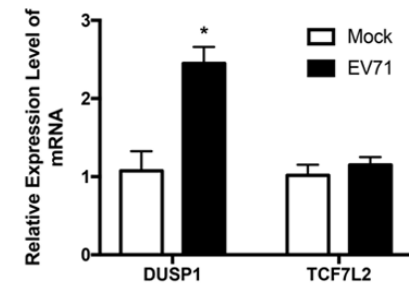
A



B



C



ceRNA network in EV71 infection

Figure 7. The qRT-PCR analysis to confirm expressions of predicted lncRNA, miRNA, and mRNA in EV71 infected RD cells. A. The lncRNA relative expression levels in EV71 infected RD cells. B. The miRNA relative expression levels in EV71 infected RD cells. C. The relative expression levels of potential target genes of miR-194-5p in EV71 infected RD cells.

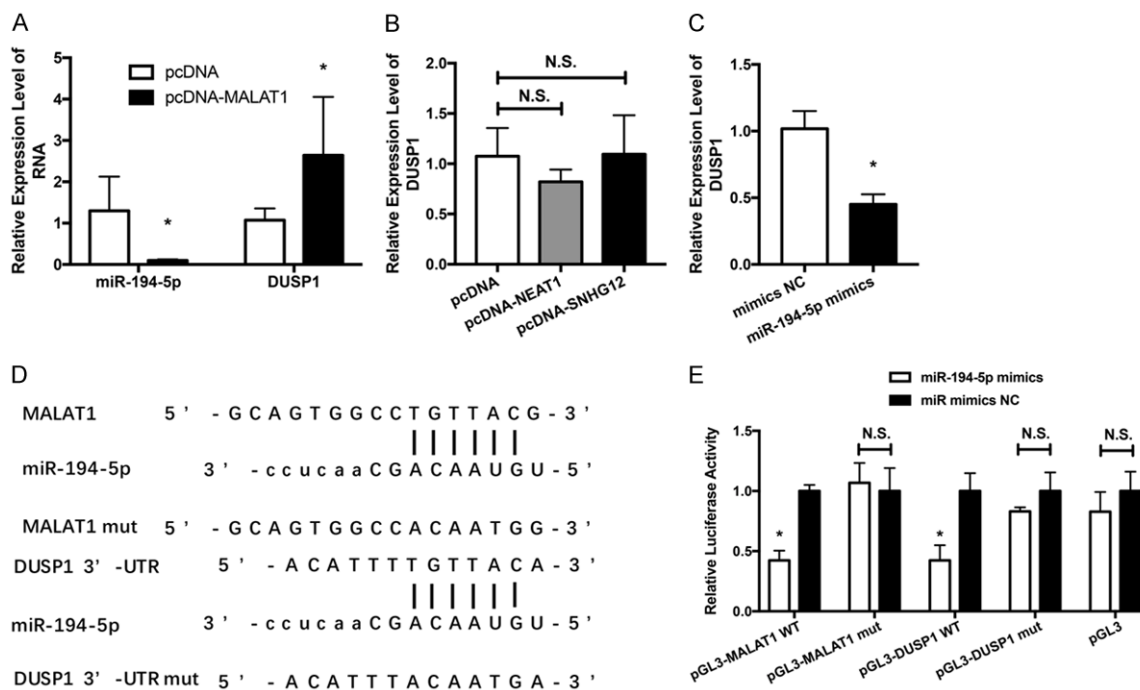


Figure 8. Validation of the putative MALAT1/miR-194-5p/DUSP1 ceRNA axis for EV71 infection. A. The regulation effect of NEAT1 and SNHG12 on DUSP1 expression. B. The regulation effect of MALAT1 on miR-194-5p and DUSP1 expression. C. The regulation effect of miR-194-5p on DUSP1 expression. D. A diagram of the binding sites of miR-194-5p on both lncRNA MALAT1 and 3'-UTR of DUSP1, suggesting a MALAT1/miR-194-5p/DUSP1 regulatory axis in EV71 infection. E. The luciferase reporter assay for combination between miR-194-5p with MALAT1 or 3'-UTR of DUSP1. The N.S. indicates no significance.

Thus, the identification of key factors involved in the regulation of apoptosis, autophagy, and other associated activities is very important to unravel the pathogenesis of EV71 infection.

Previous studies have shown that the lncRNA-miRNA-mRNA network plays a key role in the pathogenesis of viral infectious diseases [6]. Transcriptomics studies have previously revealed differential expression of a large number of lncRNA during EV71 infection [10-12]. Liao et al. [9] reported that increased expression of lnc-IRAK3-3 acted as a sponge for miR-891b, which further regulated GADD45b expression and affected cell apoptosis during EV71 infection. These evidences suggested that lncRNA-miRNA-mRNA regulatory axis mediated apoptosis or autophagy might play critical regulatory roles in the pathogenesis of EV71 infection.

In the present study, ceRNA regulatory networks were constructed for EV71 infected RD cells. The results of the analysis showed that 4 lncRNAs might act as sponges for 13 miRNAs and thus regulate the expression of 77 target genes. These results were confirmed by the overexpression of lncRNA NEAT, SNHG12, and MALAT1 in RD cells. Through experimental verification, we proved a ceRNA axis MALAT1/miR-194-5p/DUSP1 involved in EV71 infected RD cells. Several previous studies have reported the role of the MALAT1/miR-194-5p regulatory axis in various other diseases. For example, Bhattacharyya et al. [20] reported that flavivirus infection was associated with the up-regulation of MALAT1 in infected cells, which eventually resulted in cell apoptosis. In a separate study for LPS-induced acute lung injury, Nan et al. [21] reported that MALAT1 promoted apoptosis in pulmonary alveolar epithelial cells

ceRNA network in EV71 infection

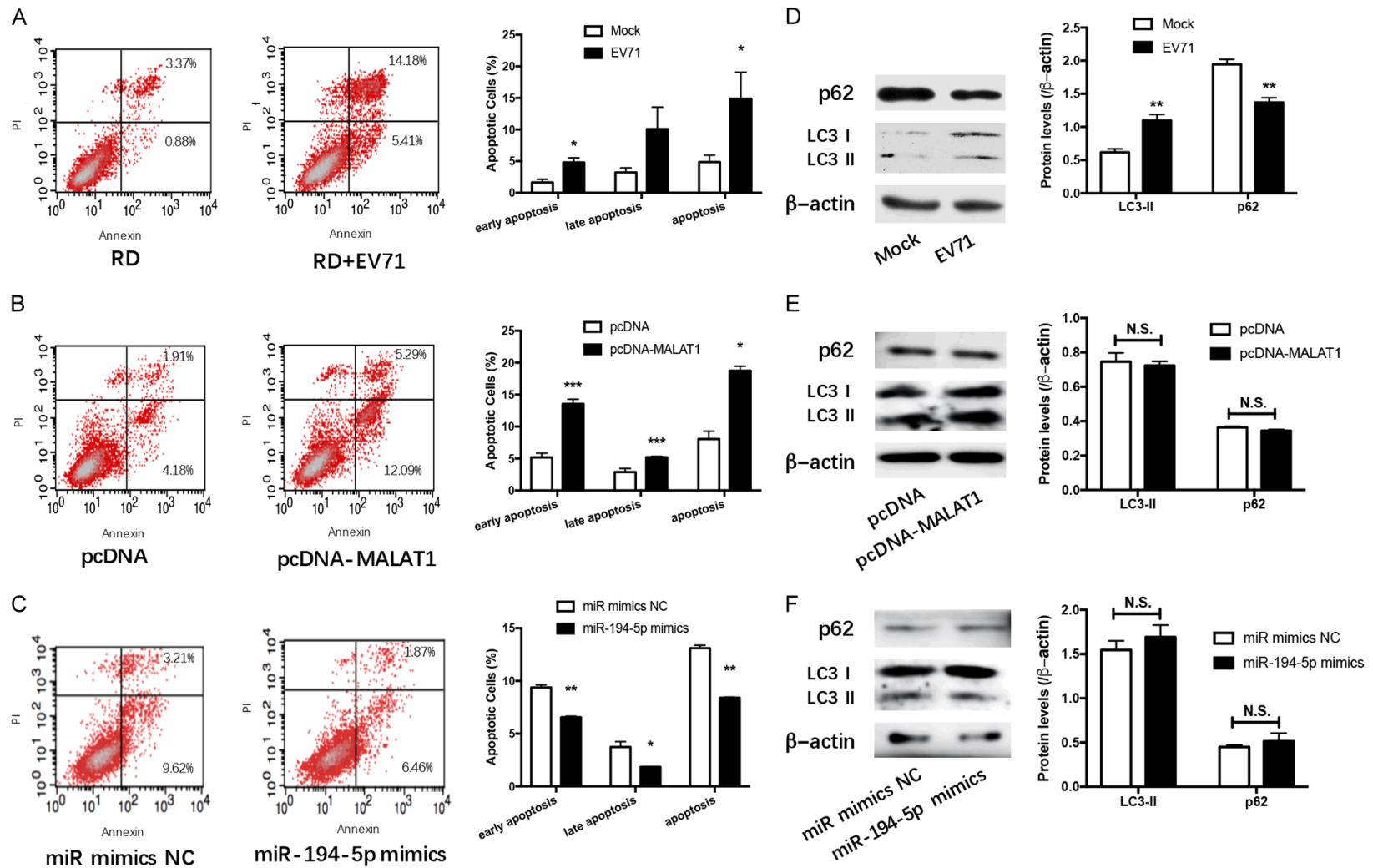


Figure 9. Detection of apoptosis and autophagy in RD cells with EV71 infection. A. The effect of EV71 infection on apoptosis of RD cells. B. The effect of lncRNA MALAT1 overexpression on apoptosis of RD cells. C. The effect of miR-194-5p mimics on apoptosis of RD cells. D. The LC3-II and p62 protein levels induced by EV71 infection in RD cells. E. The LC3-II and p62 protein levels induced by MALAT1 overexpression in RD cells. F. The LC3-II and p62 protein levels induced by miR-194-5p overexpression in RD cells. The N.S. indicates no significance.

by targeting miR-194-5p. In comparison to this, MALAT1 acted as a sponge for miR-194-5p and inhibited cellular apoptosis in the case of hypopharyngeal squamous cell carcinoma [22] and clear cell kidney cancer cells [23]. Thus, the MALAT1/miR-194-5p regulatory axis plays a pivotal but complex regulatory role in cellular apoptosis. In the present study, MALAT1/miR-194-5p axis was shown to induce apoptosis, which might mediate the pathogenesis of EV71 infection.

Several studies reported that apoptosis aggravates the development of HFMD [24]. Zhu et al. [25] showed that the deletion of Bcl2/adenovirus E1B protein-interacting protein 3 (BNIP3) improved HFMD in mice. This amelioration of EV71-induced HFMD was shown to be mediated via a reduction in cellular apoptosis. In a recent study, You et al. [26] revealed a distinct mechanism for EV71 mediated induction of neuronal apoptosis and autophagy. These EV71 mediated effects involved binding of the non-structured protein 3D of EV71 to peroxisomal protein acyl-CoA oxidase 1 (ACOX1), which was followed by downregulation of ACOX1. This might be associated with neurological complications observed in the case of HFMD. In RD cells, inhibition of apoptosis resulted in a reduction in the release of EV71 particles [27]. Thus, it is reasonable to speculate that apoptosis might promote the development of HFMD due to the prolonged course of the disease.

The autophagy was a cellular degradation mechanism induced by EV71 infection [28], which could restrict EV71 infection or promote EV71 replication [29-31]. In this study, EV71 induced LC3-II accumulation and p62 degradation, indicating the activation of autophagy. Although MALAT1/miR-194-5p regulatory axis was activated by EV71 infection, it had no effects on LC3-II and p62 protein levels, indicating that the autophagy induced by EV71 infection was mediated by other mechanism but not MALAT1/miR-194-5p regulatory axis.

This research has some limitations, but it also has certain application prospects. First, in order to ensure the reliability of prediction, we only selected the data from RD cell line rather than other cell lines, which inevitably limited the application of ceRNA networks in HFMD. Second, since miRNAs in seral exosomes have

great potential for diagnostic value [32], the lncRNAs and miRNAs predicted in the present study may be considered as biomarkers for HFMD diagnosis. However, it needs seral samples from HFMD patients for further exploration.

In summary, the transcriptome sequencing data obtained from GEO database were analyzed using various bioinformatics tools. GO, KEGG and GSEA analyses for EV71 infected RD cells revealed enrichment of DEGs mainly in cytoplasmic vesicle lumen, transmembrane transport process and TNF-signaling. The ceRNA regulatory networks were constructed on the basis of lncRNA, miRNA, and mRNA. Further, a potential ceRNA regulatory axis involving MALAT1/miR-194-5p/DUSP1 was identified, and MALAT1/miR-194-5p axis might mediate EV71 induced apoptosis. The results of the study might provide potential leads to unravel the pathogenic mechanism involved in EV71 infection, and further aid in the development of biomarkers and targeting drugs for the diagnosis and treatment of HFMD.

Acknowledgements

We are grateful to Key Project of Natural Science Foundation of Shaanxi Province (grant number 2013J2010).

Disclosure of conflict of interest

None.

Address correspondence to: Huizhong Zhang and Ke Dong, Department of Medical Laboratory and Research Center, Tangdu Hospital, Air Force Medical University, Xinsi Road No. 569, Xi'an 710038, Shaanxi, China. E-mail: huizz328@163.com (HZZ); tdjyk3@fmmu.edu.cn (KD)

References

- [1] Puenpa J, Wanlapakorn N, Vongpunsawad S and Poovorawan Y. The history of enterovirus A71 outbreaks and molecular epidemiology in the asia-pacific region. *J Biomed Sci* 2019; 26: 75.
- [2] Zhou Y, Van Tan L, Luo K, Liao Q, Wang L, Qiu Q, Zou G, Liu P, Anh NT, Hong NTT, He M, Wei X, Yu S, Lam TT, Cui J, van Doorn HR and Yu H. Genetic variation of multiple serotypes of enteroviruses associated with hand, foot and mouth disease in Southern China. *Virology* 2021; 36: 61-74.

ceRNA network in EV71 infection

- [3] Yu SB, Luo KW, Zhou YH, Dai BB, Liu FF, Yang H, Luo L, Liu J, Wang LL, Li Q, Ren LS, Liao QH and Yu HJ. Hospitalization burden of hand, foot and mouth disease in Anhua county of Hunan province, 2013-2016. *Zhonghua Liu Xing Bing Xue Za Zhi* 2019; 40: 79-83.
- [4] Esposito S and Principi N. Hand, foot and mouth disease: current knowledge on clinical manifestations, epidemiology, aetiology and prevention. *Eur J Clin Microbiol Infect Dis* 2018; 37: 391-398.
- [5] Tan YW and Chu JJH. Protecting the most vulnerable from hand, foot, and mouth disease. *Lancet Infect Dis* 2021; 21: 308-309.
- [6] Chen L, Zhou Y and Li H. LncRNA, miRNA and lncRNA-miRNA interaction in viral infection. *Virus Res* 2018; 257: 25-32.
- [7] Zhang J, Li X, Hu J, Cao P, Yan Q, Zhang S, Dang W and Lu J. Long noncoding RNAs involvement in Epstein-Barr virus infection and tumorigenesis. *Virology* 2020; 17: 51.
- [8] Zheng B, Zhou J and Wang H. Host microRNAs and exosomes that modulate influenza virus infection. *Virus Res* 2020; 279: 197885.
- [9] Liao YW, Ho BC, Chen MH and Yu SL. Host relieves lnc-IRAK3-3-sequestered miR-891b to attenuate apoptosis in enterovirus 71 infection. *Cell Microbiol* 2019; 21: e13043.
- [10] Li Y, Zhang C, Qin L, Li D, Zhou G, Dang D, Chen S, Sun T, Zhang R, Wu W, Xi Y, Jin Y and Duan G. Characterization of critical functions of long non-coding RNAs and mRNAs in rhabdomyosarcoma cells and mouse skeletal muscle infected by enterovirus 71 using RNA-seq. *Virus Res* 2018; 10: 556.
- [11] Yin Z, Guan D, Fan Q, Su J, Zheng W, Ma W and Ke C. LncRNA expression signatures in response to enterovirus 71 infection. *Biochem Biophys Res Commun* 2013; 430: 629-633.
- [12] Meng J, Yao Z, He Y, Zhang R, Yang H, Yao X, Chen L, Zhang H and Cheng J. Long non-coding RNA expression profiles in different severity EV71-infected hand foot and mouth disease patients. *Biochem Biophys Res Commun* 2017; 493: 1594-1600.
- [13] Bian L, Wang Y, Liu Q, Xia J and Long JE. Prediction of signaling pathways involved in enterovirus 71 infection by algorithm analysis based on miRNA profiles and their target genes. *Arch Virol* 2015; 160: 173-182.
- [14] Liu Y, Xu L, Lu B, Zhao M, Li L, Sun W, Qiu Z and Zhang B. LncRNA H19/microRNA-675/PPA-Ralpha axis regulates liver cell injury and energy metabolism remodeling induced by hepatitis B X protein via Akt/mTOR signalling. *Mol Immunol* 2019; 116: 18-28.
- [15] Ye W, Yao M, Dong Y, Ye C, Wang D, Liu H, Ma H, Zhang H, Qi L, Yang Y, Wang Y, Zhang L, Cheng L, Lv X, Xu Z, Lei Y and Zhang F. Remdesivir (GS-5734) impedes enterovirus replication through viral RNA synthesis inhibition. *Front Microbiol* 2020; 11: 1105.
- [16] Yao M, Dong Y, Wang Y, Liu H, Ma H, Zhang H, Zhang L, Cheng L, Lv X, Xu Z, Zhang F, Lei Y and Ye W. N(6)-methyladenosine modifications enhance enterovirus 71 ORF translation through METTL3 cytoplasmic distribution. *Biochem Biophys Res Commun* 2020; 527: 297-304.
- [17] Wang H, Yuan M, Wang S, Zhang L, Zhang R, Zou X, Wang X, Chen D and Wu Z. STAT3 regulates the type I IFN-mediated antiviral response by interfering with the nuclear entry of STAT1. *Int J Mol Sci* 2019; 20: 4870.
- [18] Tung WH, Lee IT, Hsieh HL and Yang CM. EV71 induces COX-2 expression via c-Src/PDGFR/PI3K/Akt/p42/p44 MAPK/AP-1 and NF-kappaB in rat brain astrocytes. *J Cell Physiol* 2010; 224: 376-386.
- [19] Song Y, Cheng X, Yang X, Zhao R, Wang P, Han Y, Luo Z, Cao Y, Zhu C, Xiong Y, Liu Y, Wu K and Wu J. Early growth response-1 facilitates enterovirus 71 replication by direct binding to the viral genome RNA. *Int J Biochem Cell Biol* 2015; 62: 36-46.
- [20] Bhattacharyya S and Vratil S. The malat1 long non-coding RNA is upregulated by signalling through the PERK axis of unfolded protein response during flavivirus infection. *Sci Rep* 2015; 5: 17794.
- [21] Nan CC, Zhang N, Cheung KCP, Zhang HD, Li W, Hong CY, Chen HS, Liu XY, Li N and Cheng L. Knockdown of lncRNA MALAT1 alleviates LPS-induced acute lung injury via inhibiting apoptosis through the miR-194-5p/FOXO2 axis. *Front Cell Dev Biol* 2020; 8: 586869.
- [22] Wang H, Wang F, Ouyang W, Jiang X and Li W. MALAT1 knockdown inhibits hypopharyngeal squamous cell carcinoma malignancy by targeting microRNA-194. *Oncol Lett* 2020; 20: 173-182.
- [23] Ye Y, Zhang F, Chen Q, Huang Z and Li M. LncRNA MALAT1 modified progression of clear cell kidney carcinoma (KIRC) by regulation of miR-194-5p/ACVR2B signaling. *Mol Carcinog* 2019; 58: 279-292.
- [24] Li ML, Lin JY, Chen BS, Weng KF, Shih SR, Calderon JD, Tolbert BS and Brewer G. EV71 3C protease induces apoptosis by cleavage of hnRNP A1 to promote apaf-1 translation. *PLoS One* 2019; 14: e0221048.
- [25] Zhu L, Hao X, Cao J, Xie X and Wang H. BNIP3 deletion ameliorated enterovirus 71 infection-induced hand, foot and mouth disease via inhibiting apoptosis, autophagy, and inflammation in mice. *Int Immunopharmacol* 2020; 87: 106799.
- [26] You L, Chen J, Liu W, Xiang Q, Luo Z, Wang W, Xu W, Wu K, Zhang Q, Liu Y and Wu J. Enterovirus 71 induces neural cell apoptosis and au-

ceRNA network in EV71 infection

- tophagy through promoting ACOX1 downregulation and ROS generation. *Virulence* 2020; 11: 537-553.
- [27] Xi X, Zhang X, Wang B, Wang T, Wang J, Huang H, Wang J, Jin Q and Zhao Z. The interplays between autophagy and apoptosis induced by enterovirus 71. *PLoS One* 2013; 8: e56966.
- [28] Liu ZW, Zhuang ZC, Chen R, Wang XR, Zhang HL, Li SH, Wang ZY and Wen HL. Enterovirus 71 VP1 protein regulates viral replication in SH-SY5Y cells via the mTOR autophagy signaling pathway. *Viruses* 2019; 12: 11.
- [29] Huang SC, Chang CL, Wang PS, Tsai Y and Liu HS. Enterovirus 71-induced autophagy detected in vitro and in vivo promotes viral replication. *J Med Virol* 2009; 81: 1241-1252.
- [30] Li P, Yang S, Hu D, Wei D, Lu J, Zheng H, Nie S, Liu G and Yang H. Enterovirus 71 VP1 promotes mouse Schwann cell autophagy via ER stress-mediated PMP22 upregulation. *Int J Mol Med* 2019; 44: 759-767.
- [31] Du N, Li XH, Bao WG, Wang B, Xu G and Wang F. Resveratrol-loaded nanoparticles inhibit enterovirus 71 replication through the oxidative stress-mediated ERS/autophagy pathway. *Int J Mol Med* 2019; 44: 737-749.
- [32] Barile L and Vassalli G. Exosomes: therapy delivery tools and biomarkers of diseases. *Pharmacol Ther* 2017; 174: 63-78.